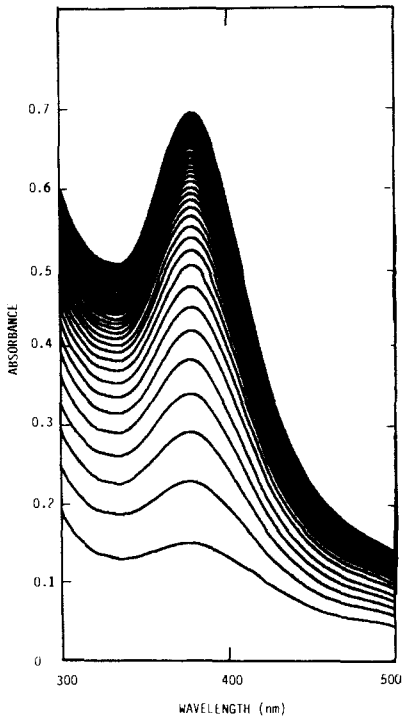

Figure 8. UV–visible absorbance spectra showing formation of the dicobalt–O-BISTREN–dioxygen complex **4** as a function of time. $T_L = {}^1/_2T_{Co} = 2.00 \times 10^{-4}$ M; $P_{O_2} = 0.21$ atm; $\mu = 0.1.00$ M (KCl); $t = 25.0$ °C. The absorbances increase with time and were measured at 1.00-min intervals.

at 95 °C may be obtained from the equilibrium studies described above. With the equilibrium concentration of dioxygen in contact with air at 95 °C, the specific rate constant, k, for the disappearance of **2** is given by eq 5. The first-order specific rate

$$k = 3.7 \times 10^{-5}/602/0.71 \times 10^{-4} = 8.6 \times 10^{-4}\ s^{-1} \quad (5)$$

constant is considerably higher than the pseudo-first-order observed rate constant because of the very low equilibrium concentration of the dioxygen complex **4** at 95 °C. Also, it is seen that the observed rate constant is second order, first order in the binuclear complex **2** and first order in dioxygen concentration.

The kinetics of formation of the dioxygen complex **4** at 25 °C from the oxygen-free binuclear complex **2** was measured spectrophotometrically, and the resulting absorbance curves are illustrated in Figure 8. The rate equation for the oxygenation reaction may be expressed by eq 6. From a plot of ln $[\mathbf{4}]/[O_2]$

$$\underset{\mathbf{2}}{Co_2(OH)L^{3+}} + O_2 \xrightarrow{k_{O_2}} \underset{\mathbf{4}}{Co_2(OH)O_2L^{3+}}$$
$$\frac{d[Co_2(OH)O_2L^{3+}]}{dt} = k_{O_2}[O_2][Co_2(OH)L^{3+}] \quad (6)$$

vs time, a second-order line with a slope $k_{O_2}([\mathbf{4}]_0 - [O_2]_0)$ was obtained. After the differences in the initial concentrations were factored out from this expression, the rate constant k_{O_2} was found to be 12.5 $M^{-1}\ s^{-1}$.

This investigation demonstrates the rapid interconversion of the monohydroxodicobalt(II)–O-BISTREN complex (**2**) and its dioxygen complex **4**. None of the binuclear cobalt(III) cryptate formed by irreversible degradation of **4** was observed from ambient temperature up to 75 °C. The irreversibly oxidized product $Co_2(OH)L^{5+}$ (**5**) formed at high temperature is not involved in this interconversion, for all practical purposes, and therefore has negligible impact on the cycling of oxygenation and deoxygenation reactions.

The rapid rate of formation of the dioxygen complex at 25.0 °C, described above, indicates that the rate of formation of the dioxygen complex **4** at elevated temperatures (ca. 40–70 °C) must be quite rapid. Also, the extensive decrease in the dioxygen complex at temperatures above ambient temperature shows that the rate of dissociation of **4** must also be rapid. Therefore, the reaction rates occuring in cycling of oxygenation and deoxygenation in aqueous solution in the 40–70 °C range should in no way be rate limiting, and the cycling time should be dependent only on the mechanics of bringing the reactants together and separating them. These facts, together with the lack of any measurable degradation reaction in this temperature range, make the cobalt–O-BISTREN complex an ideal reagent for dioxygen separation and transport. For this purpose, it seems to be more efficient and effective than any oxygen carrier previously reported.

Further work on this system will involve equilibrium and kinetics of oxygenation and deoxygenation of solid binuclear cobalt complexes of O-BISTREN and alkyl derivatives of O-BISTREN, as well as systems in which O-BISTREN is covalently attached to solids and polymer molecules.

Acknowledgment. This investigation was supported by The Robert A. Welch Foundation under research Grant A-259.

Registry No. Oxygen, 7782-44-7.

A Discrete Tetranuclear Complex of Niobium, $Nb_4Cl_{10}(PMe_3)_6$, Related to the Local Structure in $CsNb_4Cl_{11}$

F. Albert Cotton* and Maoyu Shang

Contribution from the Department of Chemistry and Laboratory for Molecular Structure and Bonding, Texas A&M University, College Station, Texas 77843. *Received April 15, 1988*

Abstract: By reaction of $Nb_2Cl_6(THT)(THF)_2$ with about a 2-fold molar ratio of Na/Hg in THF followed by addition of a moderate excess of PMe_3, the crystalline title compound is obtained. The molecule consists of two triangular Nb_3 units fused to form a centrosymmetric rhombus with outer edge lengths of 2.904 (2) and 2.934 (1) Å and an internal shortest distance of 2.987 (2) Å. There are two capping Cl atoms on opposite sides of the Nb_4 plane, a bridging Cl atom on each outer edge, and a set of ten terminal ligands consisting of four Cl atoms and six phosphine molecules. There are ten electrons available for cluster bonding and we assign five Nb–Nb single bonds. The Nb–Nb distances are similar to those in Nb_3 clusters having Nb–Nb bond orders of unity. The principal crystallographic data are as follows: space group $P2_1/n$, $a = 10.673$ (5) Å, $b = 13.582$ (4) Å, $c = 17.972$ (6) Å, $\beta = 96.16$ (3)°, $V = 2590$ (1) Å^3, $Z = 2$.

Recent work[1] in this laboratory has shown that it is possible to prepare trinuclear Nb_3 and Ta_3 cluster compounds containing equilateral triangular metal atom clusters having one capping Cl atom, three edge-bridging Cl atoms, and an assortment of Cl and

0002-7863/88/1510-7719$01.50/0

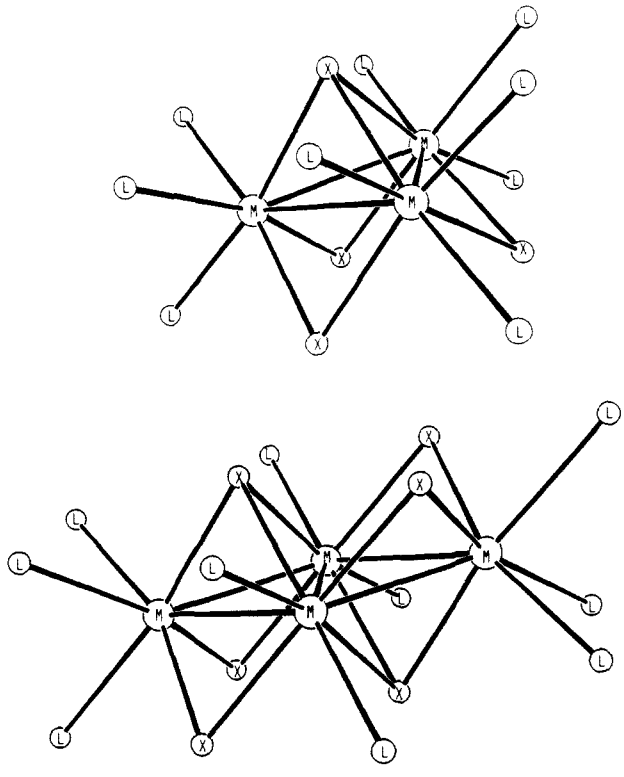

Figure 1. Schematic drawings of two important types of metal atom cluster species. In these drawings X is used for the bridging or capping ligands (but all X need not be of the same identity) and L is used for all of the peripheral ligands (and, again, need not all be the same). (a) Upper: The $M_3X_4L_9$ type. (b) Lower: The $M_4X_6L_{10}$ type.

phosphine ligands filling the nine outer positions about the central M_3X_4 unit. This type of unit is illustrated schematically in Figure 1a. It is also well-known for the elements molybdenum and tungsten where the ligands X are usually O, S, or a mixture of both.[2] With regard to niobium, one of the most interesting things about this type of cluster is that it is the local unit of structure from which Nb_3Cl_8, an infinite-array type of solid-state compound, is built up. In this case the cluster is a seven-electron system, but it can also occur with six or eight electrons occupying molecular orbitals that contribute to metal–metal bonding. The electronic structures of the trinuclear species have been discussed in some detail.[1]

We now report the preparation and structural characterization of a tetraniobium cluster compound with a structure of the type shown in Figure 1b. Although less common, this type of structure is also known in a few other cases. Moreover, it too is analogous to the local unit of structure in an extended-array type of solid-state niobium compound, namely, $CsNb_4Cl_{11}$.

Experimental Section

All preparative work was carried out under an atmosphere of argon by using standard Schlenk and vacuum line techniques or in a nitrogen-filled drybox. $NbCl_5$ was purchased from AESAR, and tetrahydrothiophene (THT) was purchased from Fluka and distilled prior to use. All solvents were freshly distilled under nitrogen from appropriate drying agents. $Nb_2Cl_6(THT)(THF)_2$[3] and $NbCl_4(THF)_2$[4] were prepared by literature methods. Stock sodium amalgam, prepared by dissolving 0.46 g of sodium in 20 mL of well-degassed mercury, was assumed to have a concentration of 1 mmol of Na/mL and handled by a syringe. A Perkin-Elmer 783 spectrophotometer was used for IR spectroscopy.

Preparation. Sodium amalgam (6.0 mL, 6.0 mmol) was added to a 70-mL THF solution of $Nb_2Cl_6(THT)(THF)_2$ (2.46 g, 4 mmol) and PMe_3 (1.4 mL, 14.8 mmol). The solution was stirred for 10 h. The color of the solution changed gradually from purple to dark brown, and a small quantity of brown precipitate was formed, which was separated along with mercury by filtration through Celite. The filtrate was layered with hexane (50 mL). Over a period of several days a fine brown powder or an oily substance, followed by some dark-colored crystals, deposited on the walls of the vessel. After a second filtration and several days of standing, dark brown platelike crystals (0.3 g, yield 11%) were obtained. After the first crop was filtered out, the filtrate was reduced in volume to half. Relayering with another 50-mL portion of hexane gave the second crop of crystals (ca. 0.1 g) along with a brown precipitate.

IR (Nujol mull, mineral oil, cm^{-1}): 1410 (w), 1270 (m), 952 (s), 852 (w), 663 (m).

Different combinations of starting materials and reaction media have been tried, such as $Nb_2Cl_6(THT)(THF)_2$ in toluene, $NbCl_4(THF)_2$ in toluene, benzene, or THF. The dried crystalline products from these reactions had the same IR spectrum, but such procedures gave inferior yields.

Table I. Crystal Data for $[Nb_4Cl_{10}(PMe_3)_6]\cdot 2THF$

formula	$Nb_4Cl_{10}P_6O_2C_{26}H_{70}$
formula weight	1326.84
space group	$P2_1/n$
systematic absences	$0k0$, $k = 2n$; $h0l$, $h + l = 2n$
a, Å	10.673 (5)
b, Å	13.582 (4)
c, Å	17.972 (6)
α, deg	90.0
β, deg	96.16 (3)
γ, deg	90.0
V, Å^3	2590 (1)
Z	2
d_{calcd}, g/cm^3	1.701
crystal size, mm	0.2 × 0.1 × 0.05
μ(Mo Kα), cm^{-1}	15.546
data collection instrument	CAD-4
radiation (monochromated in incident beam)	MoKα (λ_α = 0.71073 Å)
orientation reflections, no., range (2θ)	25, 30–34
temp, °C	22
scan method	ω–2θ
data collection range, 2θ, deg	2–46
no. of unique data, total with $F_o^2 > 3\sigma(F_o^2)$	3364, 2111
no. of parameters refined	192
trans factors, max, min	1.0, 0.793
R^a	0.052
R_w^b	0.063
quality-of-fit indicator^c	1.541
largest shift/esd, final cycle	0.09
largest peak, e/Å^3	0.848

$^a R = \sum||F_o| - |F_c||/\sum|F_o|$. $^b R_w = [\sum w(|F_o| - |F_c|)^2/\sum w|F_o|^2]^{1/2}$; $w = 1/\sigma^2(|F_o|)$. ^{c} Quality of fit $= [\sum w(|F_o| - |F_c|)^2/(N_{obsd} - N_{parameters})]^{1/2}$.

X-ray Crystallography. The air-sensitive crystals were examined under a layer of sodium-treated mineral oil, and several were sealed in capillary tubes. Routine procedures[5] were followed for crystallographic characterization and the collection of intensity data. Pertinent data are listed in Table I. There was significant decay of the crystal during data collection (ca. 45%), and an anisotropic decay correction, based on the time variation of three standards that were monitored every 2 h, was applied. In addition the usual Lp corrections and an empirical absorption correction[6] based on azimuthal scans of seven strong reflections with Eulerian χ angle near 90° were applied.

The positions of the two crystallographically independent niobium atoms in the centrosymmetric molecule were derived from a Patterson map. The remaining non-hydrogen atoms were then found by an alternating series of least-squares refinements and Fourier syntheses. The THF molecules appear to be disordered in such a way that unambiguous identification of the oxygen atom was not possible. A single choice was made based on interatomic distances, packing considerations, and thermal

(1) Cotton, F. A.; Diebold, M. P.; Feng, X.; Roth, W. J. *Inorg. Chem.* **1988**, *27*, 3413 and earlier references therein.
(2) Cotton, F. A.; Wilkinson, G. *Advanced Inorganic Chemistry*, 5th ed.; Wiley: New York, 1988; pp 825–833.
(3) Cotton, F. A.; Diebold, M. P.; Roth, W. J. *J. Am. Chem. Soc.* **1987**, *109*, 5506.
(4) Manzer, L. E. *Inorg. Chem.* **1977**, *3*, 525.
(5) (a) Bino, A.; Cotton, F. A.; Fanwick, P. E. *Inorg. Chem.* **1979**, *18*, 3558. (b) Cotton, F. A.; Frenz, B. A.; Deganello, G.; Shaver, A. J. *J. Organomet. Chem.* **1973**, *50*, 227. (c) Crystallographic computing was done on a MicroVAX computer (MicroVMX V4.5).
(6) North, A. C. T.; Phillips, D. C.; Mathews, F. S. *Acta Crystallogr., Sect. A: Cryst. Phys., Diffr., Theor. Gen. Crystallogr.* **1986**, *A24*, 351.

Table II. Positional and Isotropic Equivalent Thermal Parameters for $[Nb_4Cl_{10}(PMe_3)_6]\cdot 2THF$[a]

atom	*x*	*y*	*z*	*B*, Å^2
Nb(1)	0.3360 (1)	−0.03164 (8)	0.39190 (6)	2.66 (2)
Nb(2)	0.5647 (1)	0.07210 (8)	0.45432 (6)	2.52 (2)
Cl(1)	0.5431 (3)	−0.1104 (2)	0.4325 (2)	2.96 (7)
Cl(2)	0.2164 (3)	−0.0261 (3)	0.5010 (2)	3.80 (7)
Cl(3)	0.3678 (3)	0.1461 (2)	0.3888 (2)	3.29 (7)
Cl(4)	0.2625 (4)	−0.1981 (2)	0.3566 (2)	4.42 (8)
Cl(5)	0.6644 (3)	0.0857 (3)	0.3347 (2)	4.58 (8)
P(1)	0.1071 (3)	0.0275 (3)	0.3356 (2)	3.70 (8)
P(2)	0.4052 (4)	−0.0472 (3)	0.2516 (2)	4.38 (9)
P(3)	0.6265 (3)	0.2621 (2)	0.4533 (2)	3.57 (8)
C(1)	−0.015 (1)	−0.067 (1)	0.333 (1)	6.0 (4)
C(2)	0.041 (1)	0.126 (1)	0.3897 (8)	5.0 (4)
C(3)	0.080 (2)	0.080 (1)	0.2410 (8)	6.7 (4)
C(4)	0.422 (1)	0.067 (1)	0.1971 (9)	5.5 (4)
C(5)	0.288 (2)	−0.115 (1)	0.1850 (9)	7.0 (5)
C(6)	0.547 (1)	−0.118 (1)	0.2397 (9)	5.7 (4)
C(7)	0.795 (1)	0.2892 (9)	0.4693 (8)	4.3 (3)
C(8)	0.556 (2)	0.344 (1)	0.5183 (9)	5.8 (4)
C(9)	0.583 (2)	0.321 (1)	0.3603 (8)	5.9 (4)
O	0.682 (2)	0.056 (2)	0.063 (1)	16.9 (7)[b]
C(10)	0.645 (2)	0.143 (2)	0.018 (1)	12.7 (8)[b]
C(11)	0.654 (2)	0.222 (2)	0.069 (1)	11.2 (7)[b]
C(12)	0.738 (2)	0.190 (2)	0.135 (1)	8.6 (5)[b]
C(13)	0.763 (2)	0.088 (2)	0.124 (1)	9.2 (6)[b]

[a] Anisotropically refined atoms are given in the form of the equivalent isotropic displacement parameter defined as $(4/3)[a^2\beta_{11} + b^2\beta_{22} + c^2\beta_{33} + ab(\cos\gamma)\beta_{12} + ac(\cos\beta)\beta_{13} + bc(\cos\alpha)\beta_{23}]$. [b] These atoms were refined isotropically.

parameters. The final difference electron density map had no significant features other than three small peaks very close to the niobium atoms.

Results and Discussion

The structure of the cluster molecule, with the atom-labeling scheme defined, is shown in Figure 2. It resides on a crystallographic inversion center and thus the Nb_4 rhombus is strictly planar. It is clearly a structure of the type shown in Figure 1b. The principal interatomic distances and angles are given in Table III.

It can be seen that the Nb–Nb distances are all such that five Nb–Nb single bonds may be assumed to exist: four around the periphery and one from Nb(2) to Nb(2)′. There are, indeed, enough cluster electrons present to form these bonds. From four Nb atoms there is a total of 20 valence electrons, from which 10 must be subtracted to form the Nb–Cl bonds. The remaining 10 are used to form the five Nb–Nb bonds. The two types of peripheral bonds are nearly equal in length, viz., 2.904 (2) and 2.934 (1) Å, and these two distances are somewhat shorter than those found in the six-electron trinuclear cluster $[Nb_3Cl_{10}(PEt_3)_3]^-$, 2.976 (6) Å. The Nb(2)–Nb(2)′ bond is a little bit longer, 2.987 (2) Å. The disparity in the lengths of peripheral bonds versus the internal bond may be related to the fact that the Nb(1) and Nb(1)′ atoms each participate in only two Nb–Nb bonds and might be assigned formal oxidation numbers of III, whereas the Nb(2) and Nb(2)′ atoms each participate in three Nb–Nb bonds and may be assigned formal oxidation numbers of II. These formal oxidation number assignments are consistent with the overall mean oxidation state of the metal atoms (10/4 = 2.5) as well as with providing for each metal–metal bond to be formed in homopolar fashion (that is, with one electron from each metal atom). There is, of course, no hard and fast requirement for the latter provision, but it seems likely to be a realistic one.

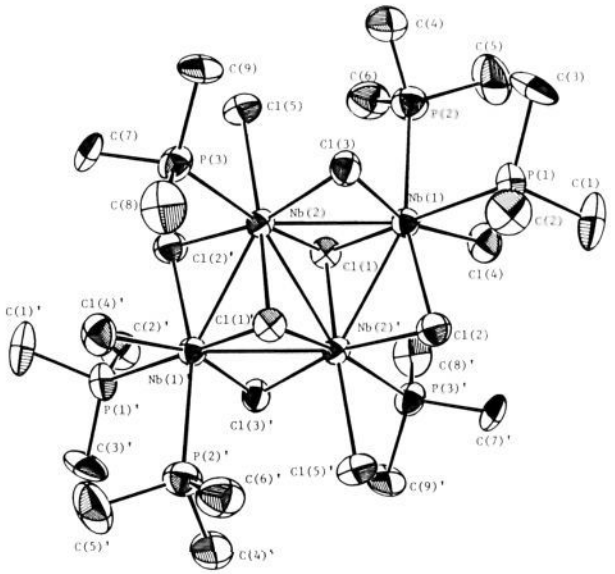

Figure 2. ORTEP drawing of the complete $Nb_4Cl_{10}(PMe_3)_6$ molecule, showing the atom-labeling scheme. Atoms are represented by their thermal ellipsoids drawn at the 30% probability level.

This general type of structure is interesting from several points of view. To begin with, we observe that it consists, in a sense, of two of the trinuclear units shown in Figure 1a fused together in such a way that the capping ligand atoms lie on opposite sides of the M_4 plane. Thus, it represents a logical first extension of the M_3 cluster structure. As we shall note later, the pattern can be extended without limit.

This general structure of the $M_4X_{10}L_6$ (or even more generically, M_4X_{16}) type has been observed previously in several cases. The most prominent examples are provided by some $[Ti(OR_4]_4$

Table III. Important Bond Distances (Å) and Angles (deg) for $[Nb_4Cl_{10}(PMe_3)_6]\cdot 2THF$[a]

atom 1	atom 2	distance	atom 1	atom 2	distance	atom 1	atom 2	distance
Nb(1)	Nb(2)	2.934 (1)	Nb(1)	Cl(4)	2.454 (3)	Nb(2)	Cl(1)′	1.497 (3)
Nb(1)	Nb(2)′	2.904 (2)	Nb(1)	P(1)	2.666 (4)	Nb(2)	Cl(2)′	2.468 (3)
Nb(1)	Cl(1)	2.493 (3)	Nb(1)	P(2)	2.711 (4)	Nb(2)	Cl(3)	2.506 (3)
Nb(1)	Cl(2)	2.454 (4)	Nb(2)	Nb(2)′	2.987 (2)	Nb(2)	Cl(5)	2.506 (4)
Nb(1)	Cl(3)	2.440 (3)	Nb(2)	Cl(1)	2.516 (3)	Nb(2)	P(3)	2.664 (3)

atom 1	atom 2	atom 3	angle	atom 1	atom 2	atom 3	angle	atom 1	atom 2	atom 3	angle
Nb(2)	Nb(1)	Nb(2)′	61.54 (4)	Cl(4)	Nb(1)	P(1)	85.7 (1)	Cl(1)	Nb(2)	P(3)	86.6 (1)
Cl(1)	Nb(1)	Cl(2)	107.5 (1)	Cl(4)	Nb(1)	P(2)	78.4 (1)	Cl(2)	Nb(2)	Cl(3)	166.2 (1)
Cl(1)	Nb(1)	Cl(3)	108.1 (1)	P(1)	Nb(1)	P(2)	90.0 (1)	Cl(2)	Nb(2)	Cl(5)	79.8 (1)
Cl(1)	Nb(1)	Cl(4)	85.9 (1)	Nb(1)	Nb(2)	Nb(1)′	118.46 (5)	Cl(2)	Nb(2)	P(3)	91.2 (1)
Cl(1)	Nb(1)	P(1)	171.1 (1)	Nb(1)	Nb(2)	Nb(2)′	58.73 (4)	Cl(3)	Nb(2)	Cl(5)	88.8 (1)
Cl(1)	Nb(1)	P(2)	85.3 (1)	Cl(1)	Nb(2)	Cl(1)′	106.9 (1)	Cl(3)	Nb(2)	P(3)	78.7 (1)
Cl(2)	Nb(1)	Cl(3)	94.2 (1)	Cl(1)	Nb(2)	Cl(2)′	82.5 (1)	Cl(5)	Nb(2)	P(3)	78.1 (1)
Cl(2)	Nb(1)	Cl(4)	93.2 (1)	Cl(1)	Nb(2)	Cl(3)	105.3 (1)	Nb(1)	Cl(1)	Nb(2)	71.72 (8)
Cl(2)	Nb(1)	P(1)	76.1 (1)	Cl(1)	Nb(2)	Cl(5)	88.8 (1)	Nb(1)	Cl(1)	Nb(2)′	71.19 (9)
Cl(2)	Nb(1)	P(2)	164.4 (1)	Cl(1)	Nb(2)	P(3)	166.3 (1)	Nb(2)	Cl(1)	Nb(2)′	73.15 (9)
Cl(3)	Nb(1)	Cl(4)	161.3 (1)	Cl(1)	Nb(2)	Cl(2)′	106.9 (1)	Nb(1)	Cl(2)	Nb(2)′	72.3 (1)
Cl(3)	Nb(1)	P(1)	79.4 (1)	Cl(1)	Nb(2)	Cl(3)	82.1 (1)	Nb(1)	Cl(3)	Nb(2)	72.77 (9)
Cl(3)	Nb(1)	P(2)	90.2 (1)	Cl(1)	Nb(2)	Cl(5)	163.5 (1)				

[a] Numbers in parentheses are estimated standard deviations in the least significant digits.

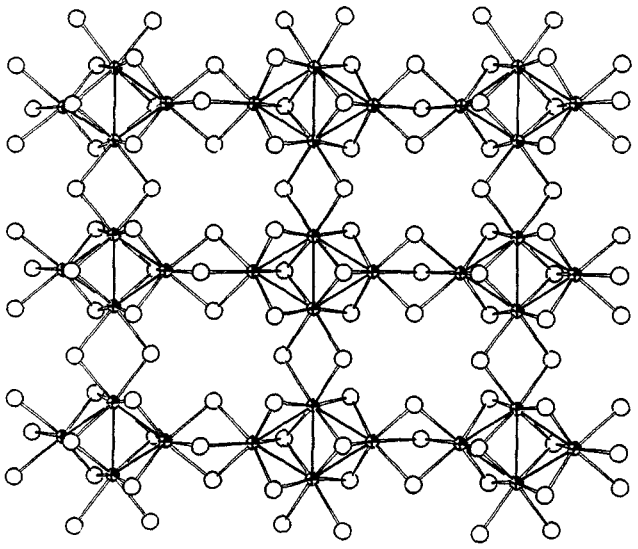

Figure 3. A view of the $CsNb_4Cl_{11}$ structure, with the Cs^+ ions omitted. Small spheres are Nb atoms and larger ones Cl atoms.

molecules[7] where there are no metal–metal bonds, by a tetranuclear Mo(V) molecule in which there are only two, isolated Mo–Mo bonds,[8] by molecular $W_4(OEt)_{16}$,[9] and by some subunits found in some mixed oxides of molybdenum in its lower oxidation states.[10] In the tungsten and one type of molybdenum cluster there are only eight electrons instead of ten for cluster bonding and the structure is distorted so that the peripheral bonds are alternately long and short, while the internal bond remains short. It has been shown that this is a predictable result of the operation of a second-order Jahn–Teller effect.[11]

The most important prior example of this sort of structure, insofar as its relationship to the present compound is concerned, is found in $CsNb_4Cl_{11}$ (and related compounds with Rb in place of Cs and Br in place of Cl).[12] The structure of this substance is shown in Figure 3, where it is easily seen that it consists of an infinite array of M_4X_{16} units fused together. The Cl atoms are not in a hexagonal close-packed array (as they are, approximately, in Nb_3Cl_8) but the orthorhombic arrangement is somewhat similar, creating octahedral holes in which the Nb atoms reside in an ordered pattern that gives rise to the Nb_4 clusters. Here, again, there are ten electrons available for cluster bonding and the internal bond is longer (2.95 Å) than the peripheral ones (2.84 Å).

Extensions of the Structural Pattern. The fusion of two triangular units to form a rhombus, as exemplified by the progression from the $Nb_3Cl_4L_9$ type structure (Figure 1a) to the $Nb_4Cl_6L_{10}$ type (Figure 1b), is a step that can be repeated over and over again, to produce either odd- or even-membered finite arrays (Figure 4a,b) or an infinite array (Figure 4c). If there is to be a full two-electron bond between every adjacent pair of metal atoms, it is easily seen that for an N-nuclear array each metal atom will have to supply $4 - (6/N)$ electrons. In the case of the rhomboidal unit described here this expression gives a mean oxidation state of $4 - (6/4) = 2.5$. This is, of course, in agreement with the molecular formula $Nb_4Cl_{10}(PMe_3)_6$. It should be pointed out that the structures shown in Figure 4 may well be stable even when fewer than $4 - (6/N)$ electrons are provided by each metal atom,

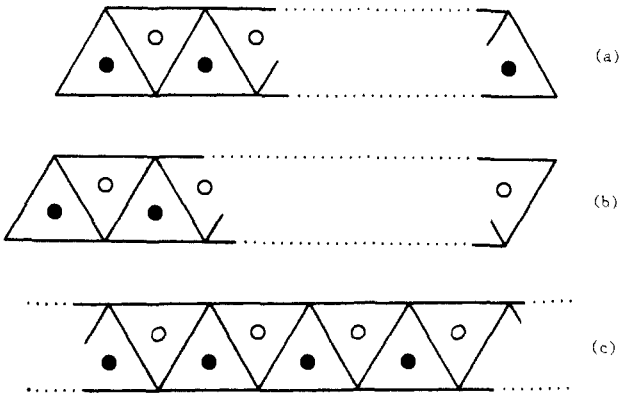

Figure 4. More extended arrays (N-mers) formed by fusion of capped equilateral triangular M_3 units. (a) N odd; (b) N even; (c) $N = \infty$.

although for an electron-defective structure the possibility of distortion must be considered. Indeed, species with $N = 4$ and only eight electrons (as we have already mentioned) provide a textbook case of second-order Jahn-Teller distortion.[11]

To the best of our knowledge, no substance containing a finite band of type a or b in Figure 4 with $4 < N < \infty$ has yet been reported, either with the full complement of $4N - 6$ electrons or with fewer. There are, however, several cases of infinite bands (Figure 4c). All of these are made up of molybdenum and oxyen atoms. As already noted,[10] the compound $Ba_{1.14}Mo_8O_{16}$ contains two kinds of rhomboidal Mo_4 clusters, one with ca. ten electrons and an essentially equal set of five Mo–Mo bonds and the other with ca. eight electrons and a distorted rhomboidal shape. However, these Mo_4 clusters occur in infinite strips such that if more electrons were available to make additional Mo–Mo bonds, one could imagine the separate Mo_4 rhombuses joining together into infinite chains of the type shown in Figure 4c.

The only true example of the infinite band structure depicted in Figure 4c appears to be found in $NaMo_2O_4$, where all Mo–Mo distances parallel to the run of the chain are equal (2.89 Å) and all cross bonds are equal (2.54 Å).[13] These chains are markedly electron deficient, however. Instead of the $4 - (6/\infty) = 4$ electrons per Mo atom necessary to form single bonds between all adjacent pairs of Mo atoms, there are only 2.5 electrons per Mo atom. Clearly, from the marked disparity in the lengths of the two kinds of Mo–Mo closest neighbors, these electrons are not distributed equally so as to form equivalent bonds of order $^5/_8$. McCarley and co-workers have suggested that the cross bonds are approximately full single bonds while the ones along band edges are of order 0.25 or only slightly greater. This seems an entirely reasonable allocation of the available electrons.

It is only to be expected that in oxide compounds, where each anion requires two electrons from the metal atoms present, it is not easy to devise systems with enough electrons available for metal–metal bonding to reach, or more closely approach, a full set of single bonds. However, it is possible to design structures and compositions for mixed halide (as opposed to mixed oxide) compounds where such bonding could be achieved. We are now attempting to prepare such substances.

Acknowledgment. We are grateful to The Robert A. Welch Foundation for financial support under Grant No. A-494.

Supplementary Material Available: Full tables of bond distances and angles, a stereoview, and anisotropic displacement parameters (7 pages); a table of observed and calculated structure factors (19 pages). Ordering information is given on any current masthead page.

(7) Wright, D. A.; Williams, D. A. *Acta Crystallogr., Sect. B* **1968**, *24B*, 1107.
(8) Koch, S. A.; Lincoln, S. *Inorg. Chem.* **1982**, *21*, 2904.
(9) Chisholm, M. H.; Huffman, J. C.; Leonelli, J. *J. Chem. Soc., Chem. Commun.* **1981**, 270.
(10) Torardi, C. C.; McCarley, R. E. *J. Solid State Chem.* **1981**, *37*, 393.
(11) Cotton, F. A.; Fang, A. *J. Am. Chem. Soc.* **1982**, *104*, 113.
(12) Bröll, A.; Simon, A.; Schnering, H. G. v.; Schäfer, H. *Z. Anorg. Allg. Chem.* **1969**, *367*, 1.
(13) McCarley, R. E.; Lii, K.-H.; Edwards, P. A.; Brough, L. F. *J. Solid State Chem.* **1985**, *57*, 17.